Aging-induced two-step ferroelectric-to-paraelectric transition in acceptor-doped ferroelectrics

Jinghui Gao,[1,2,3] Dezhen Xue,[1,3] Huixin Bao,[1,3] Lixue Zhang,[1] Chao Zhou,[1,2,3] Wenfeng Liu,[1,2] Wei Chen,[1,2] and Xiaobing Ren[1,3,a)]
[1]*Multi-disciplinary Materials Research Center, Xi'an Jiaotong University, Xi'an 710049, People's Republic of China*
[2]*State Key Laboratory of Electrical Insulation and Power Equipment, Xi'an Jiaotong University, Xi'an 710049, People's Republic of China*
[3]*Ferroic Physics Group, National Institute for Materials Science, Tsukuba, Ibaraki 305-0047, Japan*

(Received 8 September 2009; accepted 17 January 2010; published online 25 February 2010)

It is well known that first-order ferroelectric to paraelectric transition is a one-step transition and it gives rise to one latent heat peak and one permittivity peak during heating. In the present paper, however, we report an unexpected finding; in Mn-doped $Ba(Zr_{0.01}Ti_{0.98}Mn_{0.01})O_{3-\delta}$ the ferroelectric to paraelectric transition proceeds in two steps, after the sample has experienced a prior aging at the differential scanning calorimetry (DSC) peak temperature and followed by cooling down to a fully ferroelectric state. The two-step transition is evidenced by a split DSC peak as well as a split permittivity peak. These abnormal effects can be explained by considering that aging at DSC peak temperature corresponds to aging in a two-phase state (paraelectric+ferroelectric). Such two-phase aging produces two different defect symmetries, which give rise to different stabilities for the same ferroelectric phase and thus results in different reverse transition temperatures. © *2010 American Institute of Physics*. [doi:10.1063/1.3309697]

Ferroelectric materials are an important class of functional materials and have found a wide range of applications owing to their ferroelectricity, piezoelectricity, pyroelectricity, etc. These materials undergo a ferroelectric-paraelectric (FE→PE) transition when heated to above the Curie temperature (T_C). This transition is a first order transition with the spontaneous polarization vanishing abruptly at T_C. The discontinuity in polarization causes a discontinuity in entropy and hence yielding a latent heat at T_C,[1] which can be detected by differential scanning calorimeter (DSC). As a result, FE→PE transition gives rise to one DSC peak around T_C on heating. In this letter, however, we report an unexpected finding—FE→PE transition seems to proceed in two steps, if the sample experienced a prior aging at the DSC peak temperature and followed by subsequent cooling.

We fabricated $Ba(Ti_{0.98}Zr_{0.01}Mn_{0.01})O_{3-\delta}$ ceramic samples (δ is the oxygen vacancy) using a conventional solid-solution method. Mn^{3+} was added as B-site acceptor dopant, which creates oxygen vacancies and causes aging effect. Zr^{4+} was added to broaden the FE–PE DSC peak temperature range[2] and thus made it easier to conduct peak-temperature aging. The ferroelectric transition (PE→FE) and reverse transition (FE→PE) of the sample was monitored by a DSC Q200 calorimeter (TA Instruments) with a heating/cooling rate of 3 °C/min, and the peak temperatures for forward and reverse transition were 115.6 and 119.3 °C respectively [Fig. 1(a)]. Aging temperature was selected to be the peak temperature of FE→PE transition (119.3 °C).

It should be noted that the DSC peak temperature corresponds to a maximum transition rate of FE→PE transition; thus it corresponds to a coexistence of FE and PE phases, as shown in the inset of Fig. 1(a). Therefore, peak-temperature aging actually corresponds to a FE+PE two-phase aging. Before aging, the sample was heated to 280 °C (well above T_C) for 10 min to eliminate the preexisting aging effect. Then it was cooled to full ferroelectric state (80 °C) followed by immediate heating to the DSC peak temperature (119.3 °C) and the sample was aged at this temperature for different length of time. After the peak-aging or two-phase aging, the sample was cooled to a full ferroelectric state again (80 °C) and then heated up to a full paraelectric state during which the heat flow was recorded.

Figure 1(b) shows the evolution of DSC heating peak associated with the FE→PE transition for the peak-temperature-aged sample with different aging time (0–32 h). In contrast with the normal single peak for the unaged sample, the DSC peak of two-phase-aged sample gradually split into two peaks with increasing peak-aging time, i.e., the FE–PE transition proceeds in two-steps. The left peak (with peak temperature T_1) corresponds to the first step, and the right peak (with peak temperature T_2) corresponds to the second step. The evolution of the two peak temperature T_1 and T_2 with peak aging time is shown in Fig. 1(c). We can see that the left peak T_1 remains essentially unchanged, whereas the right peak T_2 shifts to high temperature with increasing aging time and finally saturates (feature of FE aging).

The two-step FE–PE transition can also be identified by permittivity measurement. Figures 2(a) and 2(b) shows, respectively, the ε'-T heating curve of the above sample without and with prior peak aging. It is clear after peak aging the single permittivity peak split into two.

Now we discuss the origin of the two-step FE–PE transition induced by the peak-temperature aging. As shown in the inset of Fig. 1(a) and discussed above, peak-temperature aging corresponds to the aging of a mixture of FE and PE phases. Recent studies have shown that aging in a fully FE state can cause a stabilization[3–16] of the FE phase and hence the increase in FE→PE transition temperature T_C.[17,18] Such

a)Author to whom correspondence should be addressed. Electronic mail: ren.xiaobing@nims.go.jp.

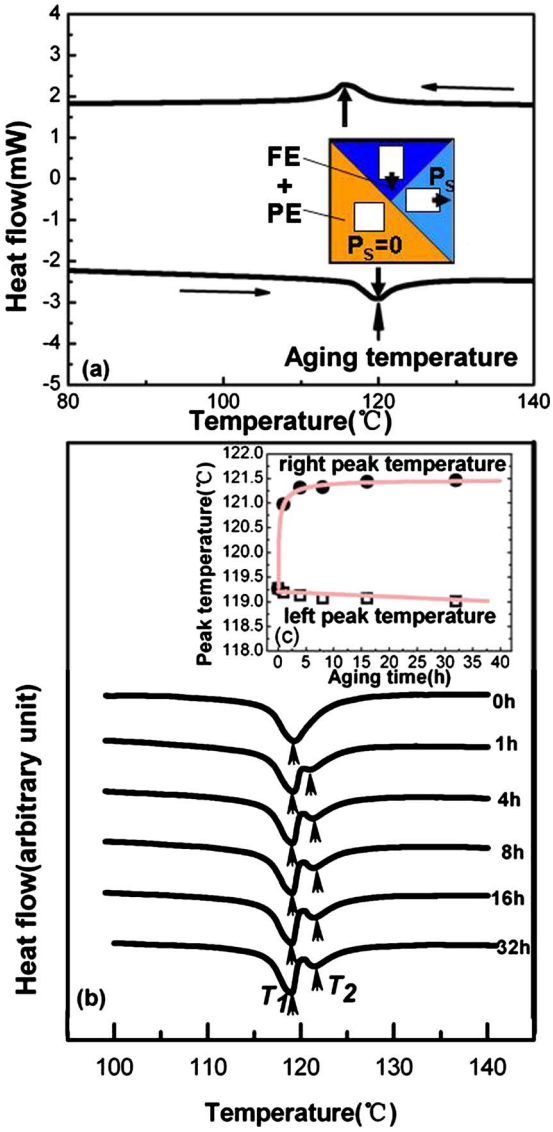

FIG. 1. (Color online) DSC curve of $Ba(Zr_{0.01}Ti_{0.98}Mn_{0.01})O_{3-\delta}$ ceramic before and after DSC-peak-temperature aging (119.3 °C). (a) DSC curve of normal ferroelectric transition and reverse transition. The inset shows DSC peak temperature corresponds to a ferroelectric+paraelectric two-phase state. (b) The DSC curve gradually splits into two peaks with the increase in DSC-peak-aging time (119.3 °C, 0–32 h). (c) The left peak T_1 and right peak T_2 temperatures as a function of aging time.

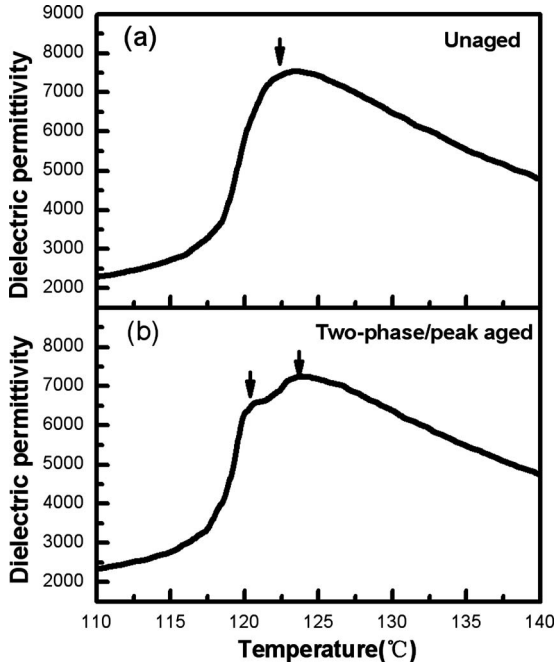

FIG. 2. Dielectric permittivity peak profile of $Ba(Zr_{0.01}Ti_{0.98}Mn_{0.01})O_{3-\delta}$ sample during heating from a full FE state to a PE state without and with two-phase aging. (a) Unaged sample. (b) Dielectric permittivity curve after two-phase-aging (119.3 °C for 32 h).

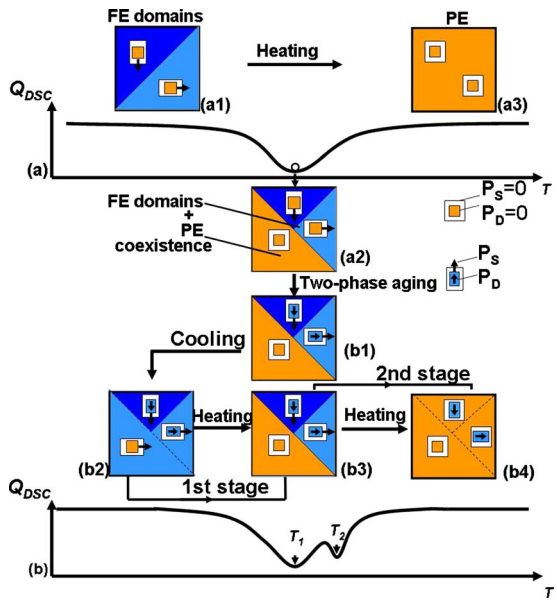

FIG. 3. (Color online) Mechanism for aging-induced two-step FE→PE transition. $\mathbf{P_S}$ and $\mathbf{P_D}$ are spontaneous and defect polarization, respectively. The large and small squares or rectangles represent different crystal symmetries and defect SRO symmetries, respectively. (a) Normal FE→PE one-step transition for unaged sample. (a1) Unaged FE phase with zero $\mathbf{P_D}$. (a2) The sample is a FE+PE two phase mixture at the DSC peak temperature. FE portion: upper half (blue-colored FE domains); PE portion: lower half (yellow-colored PE phase). (a3) PE phase after heating from unaged FE phase. (b) Two-step transition after two-phase aging. (b1) After aging in the (a2) state (FE+PE two phase mixture), the FE portion has a SRO of the polar tetragonal symmetry and a nonzero $\mathbf{P_D}$, while PE portion has a cubic SRO and a zero $\mathbf{P_D}$. (b2) The existence of two different SRO symmetries after the sample is cooled to a full FE state. (b3) On heating, the first-step FE→PE transition corresponds to the transition in the former PE portion with a zero $\mathbf{P_D}$. (b4) Second-step FE→PE transition corresponds to the transition of the former FE portion with a nonzero $\mathbf{P_D}$.

a ferroelectric stabilization effect was shown to stem from a symmetry-conforming short-range order property of point defects.[3,4,19] This is an important clue for understanding the present two-step transition due to peak aging or two-phase aging.

In the following, we shall show the evolution of defect configuration during two-phase aging and explain the origin of two-phase-aging-induced two-step FE–PE transition. In ungaged acceptor-doped ferroelectrics, oxygen vacancies[20] tend to form a cubic defect configuration (SRO symmetry)[3,4,15] and thus the whole sample has the same SRO symmetry everywhere. As the results, the unaged sample exhibits one-stage reverse ferroelectric transition [Fig. 3(a)].

Now, we heat the sample to the DSC peak temperature, i.e., the sample is composed of regions of FE and PE phases [Fig. 3(a2)]. The two phases correspond to two different crystal symmetries, cubic for PE phase and polar tetragonal for FE phase. After aging in such a two-phase state, the de-

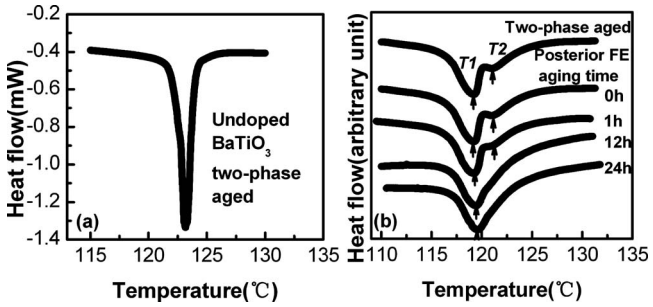

FIG. 4. Verification of the two predictions from the mechanism of two-phase aging shown in Fig. 3. (a) No DSC peak splitting for undoped $BaTiO_3$ ceramic even after two-phase aging (121.6 °C,3 h). (b) Split DSC curve of $Ba(Zr_{0.01}Ti_{0.98}Mn_{0.01})O_{3-\delta}$ caused by two-phase aging (119.3 °C,1 h) gradually changes into a normal single peak after increasing posterior FE aging time in fully ferroelectric state (100 °C).

fect SRO symmetry of each phase conforms to the crystal symmetry of the corresponding phase [Fig. 3(b1)], according to the symmetry-conforming SRO principle.[3,4] In the FE portion, the defect symmetry tends to adopt the polar tetragonal crystal symmetry, and thus forms a defect dipole $\mathbf{P_D}$ after aging.[3,4,21–23] $\mathbf{P_D}$ can stabilize the ferroelectric phase and thus increases the thermodynamic stability (and T_C) of the FE-aged portion.[17] The PE portion, on the other hand, keeps its "cubic" defect SRO symmetry after aging and the stability (or T_C) of this portion remains unchanged. Subsequent cooling the sample results in a full FE state without changing defect symmetry in the two portions [Fig. 3(b2)]. Thus the ferroelectric state is composed of two regions of different SRO symmetries and thus different thermodynamic stabilities. During the heating process from this full FE state, the FE phase formed from the former PE portion corresponds to a relatively lower T_C because its SRO symmetry (cubic) does not match its crystal symmetry (polar tetragonal). Thus this FE portion transforms into PE phase first, giving rise to the first-step FE→PE transition [Figs. 3(b2)–3(b3)]. With further heating the sample, the former FE portion, in which SRO symmetry conforms with the polar tetragonal crystal symmetry has higher T_c for the FE→PE transition; this results in the second-step FE–PE transition [Figs. 3(b3)–3(b4)]. Therefore, the two-step transition is microscopically caused by the coexistence of two different defect SRO symmetries (in different regions) after the two-phase aging. The two SRO symmetries lead to two different stabilities for the ferroelectric phase, thus result in a two-step transition. With this mechanism we can also understand that the shift of T_2 peak toward higher temperature with aging time is due to the gradual stabilization of the previous FE portion, whereas the insensitivity of T_1 to two-phase aging is due to the identical defect SRO symmetry of the previous PE portion for different aging time.

The above explanation suggests that two-step transition caused by two-phase aging stems from the existence of two different defect symmetries in the PE and FE portion of the crystal. Following this mechanism we can make two predictions: (1) The aging-induced two-step transition (i.e., peak splitting) cannot occur in systems without mobile defects; this is because defect SRO symmetry is not able to change with time in both PE and FE phases and thus it is not possible to create two different stabilities. (2) Split peak will become a single peak if the two-phase-aging is followed by a long-time aging in full FE state. This is because that long-time FE-aging changes the two different defect symmetries into the same one, following the FE crystal symmetry; thus the FE→PE transition occurs in a single step.

To verify these predictions, we performed two experiments. First, we conducted peak-temperature aging (121.6 °C) on an undoped $BaTiO_3$ ceramic, which has virtually no aging effect. The result [Fig. 4(a)] shows that there is no peak splitting on the DSC curve, verifying the first prediction. Second, we performed posterior ferroelectric aging on a two-phase aged (119.3 °C, 1 h) $Ba(Ti_{0.98}Zr_{0.01}Mn_{0.01})O_{3-\delta}$ sample for different time and then observed the FE→PE transition behavior as a function of the posterior FE aging time. The result is shown in Fig. 4(b). Without posterior FE aging the DSC peak of two-phase-aged sample exhibits a splitting during FE→PE transition. With increasing posterior aging time, the split peaks T_1 and T_2 gradually merge into one peak, i.e., becoming one step FE–PE transition; this verifies the second prediction. It should be noted that the gradual shift of T_2 toward T_1 is due to an aging-temperature effect.[17] The verification of the two predictions provide further support to the mechanism shown in Fig. 3.

In conclusion, a two-step FE→PE transition was found in acceptor-doped barium titanate system after aging at the DSC peak temperature. This effect can be ascribed to the formation of two different defect SRO symmetries in the sample during the aging in the DSC peak temperature (or FE+PE state), hence causing two different stabilities in the sample and a two-step FE→PE transition.

The authors gratefully acknowledge the support of National Natural Science Foundation of China (Grant Nos. 50720145101 and 50702042), National Basic Research Program of China (Grant Nos. 2004CB619303 and 2010CB631003), and 111 project of China.

[1] M. E. Lines and A. M. Glass, *Principles and Applications of Ferroelectrics and Related Materials* (Oxford University Press, New York, 1977).
[2] D. Hennings, A. Schnell, and G. Simon, J. Am. Ceram. Soc. **65**, 539 (1982).
[3] X. Ren, Nature Mater. **3**, 91 (2004).
[4] L. X. Zhang and X. Ren, Phys. Rev. B **71**, 174108 (2005).
[5] H. Thoman, Ferroelectrics **4**, 141 (1972).
[6] R. Lohkämper, H. Neumann, and G. Arlt, J. Appl. Phys. **68**, 4220 (1990).
[7] K. Uchino, *Ferroelectric Device* (Marcel Dekker, New York, 2000).
[8] W. A. Schulze and K. Ogino, Ferroelectrics **87**, 361 (1988).
[9] P. V. Lambeck and G. H. Jonker, J. Phys. Chem. Solids **47**, 453 (1986).
[10] U. Robels and G. Arlt, J. Appl. Phys. **73**, 3454 (1993).
[11] G. Arlt and H. Neumann, Ferroelectrics **87**, 109 (1988).
[12] D. Lin, K. W. Kwok, and H. L. W. Chan, Appl. Phys. Lett. **90**, 232903 (2007).
[13] P. V. Lambeck and G. H. Jonker, Ferroelectrics **22**, 729 (1978).
[14] Y. A. Genenko, Phys. Rev. B **78**, 214103 (2008).
[15] D. Xue, J. Gao, L. Zhang, H. Bao, W. Liu, C. Zhou, and X. Ren, Appl. Phys. Lett. **94**, 082902 (2009).
[16] M. Takahashi, Jpn. J. Appl. Phys., Part 1 **9**, 1236 (1970).
[17] D. Z. Sun, X. Ren, and K. Otsuka, Appl. Phys. Lett. **87**, 142903 (2005).
[18] M. M. Ahmad, K. Yamada, P. Meuffels, and R. Waser, Appl. Phys. Lett. **90**, 112902 (2007).
[19] X. Ren and K. Otsuka, Nature (London) **389**, 579 (1997).
[20] D. M. Smith, *The Defect Chemistry of Metal Oxide* (Oxford University Press, New York, 2000).
[21] R.-A. Eichel, P. Erhart, P. Traskelin, K. Albe, H. Kungl, and M. J. Hoffmann, Phys. Rev. Lett. **100**, 095504 (2008).
[22] W. L. Warren, G. E. Pike, K. Vanheusden, D. Dimos, B. A. Tuttle, and J. Robertson, J. Appl. Phys. **79**, 9250 (1996).
[23] L. X. Zhang, E. Erdem, X. Ren, and R. A. Eichel, Appl. Phys. Lett. **93**, 202901 (2008).